

VASCULAR COUPLING DEVICE

by

Ryan Wallace Brewster

A thesis submitted to the faculty of
The University of Utah
in partial fulfillment of the requirements for the degree of

Master of Science

Department of Mechanical Engineering

The University of Utah

May 2017

Copyright © Ryan Wallace Brewster 2017

All Rights Reserved

The University of Utah Graduate School

STATEMENT OF THESIS APPROVAL

The thesis of Ryan Wallace Brewster
has been approved by the following supervisory committee members:

<u>Bruce Kent Gale</u>	, Chair	<u>2/16/17</u> Date Approved
------------------------	---------	---------------------------------

<u>Jayant Prasad Agarwal</u>	, Member	<u>2/16/17</u> Date Approved
------------------------------	----------	---------------------------------

<u>Kenneth LaVann Monson</u>	, Member	<u>2/16/17</u> Date Approved
------------------------------	----------	---------------------------------

and by Timothy Ameal, Chair of
the Department of Mechanical Engineering

and by David B. Kieda, Dean of The Graduate School.

ABSTRACT

In performing microsurgeries, the procedure of vascular anastomosis is performed frequently. When executing this procedure, the most widely used method is hand suturing the vessels back together. This process, however, is extremely time consuming (depending on the size and location of the vessel and the experience of the surgeon) and is subject to human error. The vascular coupling device and its accompanying installation tools in this work have been designed and tested to reduce human error and significantly decrease the amount of time required to perform the anastomosis. Tests that were performed on the vascular coupling device include a pressure leak test (both open-end and sealed-end), a tensile test, and the time required to complete the anastomosis. The coupler was also installed on the carotid artery of a cadaver swine. The coupling device had significantly less leakage than hand sutured anastomoses (p values of approximately 0.05 or lower), was able to withstand an average tensile force of 5.52 ± 2.34 N (n=5) before failure, and was installed in an average of 7 min and 34 sec (n=3).

This work is dedicated to all those who do good in the world, to leave the world a better place than they find it.

TABLE OF CONTENTS

ABSTRACT.....	iii
LIST OF FIGURES	vii
ACKNOWLEDGEMENTS.....	ix
Chapters	
1. BACKGROUND	1
1.1. Hand Suturing	2
1.2. Other Anastomotic Devices.....	3
1.2.1. GEM Microvascular Anastomotic Coupler.....	3
1.2.2. Thermoreversible Intravascular Poloxamer Stent	5
1.2.3. AnastoClips	5
1.2.4. Laser Welding	6
1.3. Design Research and Potential.....	6
1.4. Prior Work	8
1.4.1. Vascular Coupling Device with 5 Spikes on Wings that Can Rotate 45°	8
1.4.2. Second Generation of Vascular Coupling Device with 4 Spikes Rotating 90°	9
1.4.3. Vascular Coupling Device Without Spikes.....	10
1.5. Thesis Overview	12
2. VASCULAR COUPLING DEVICE	13
2.1. Design of the Vascular Coupling Device	13
2.1.1. Justification of Length of Inner Ring Wall/Spacing Between Inner and Outer Rings.....	15
2.2. Design of the Installation Tools.....	20
2.2.1. Previous Installation Tools.....	20
2.2.2. Modified Installation Tools	22
2.3. Selection of Materials.....	24
2.3.1. Materials of the Coupler.....	24
2.3.2. Materials of the Installation Tools.....	26
2.4. Testing Protocol	27
2.4.1. Leak Tests.....	28
2.4.2. Tensile Test	29
2.4.3. Time for Anastomosis	30

2.5. Testing Results and Discussion	31
2.5.1. Leak Tests Results and Discussion	31
2.5.2. Tensile Test Results and Discussion	36
2.5.3. Time for Anastomosis Results and Discussion	40
2.6. Cadaver Animal Study	42
3. SUPPORTING MATERIALS	45
3.1. Design Requirements for the Biodegradable Vascular Coupling Device	45
3.2. 3D Printing.....	45
3.3. Mechanical Properties of PLA	47
3.3.1. Mechanical Properties of PLDLA	49
3.4. Sterilization.....	50
4. CONCLUSIONS.....	51
4.1. Conclusions	51
4.2. Contributions	53
4.2.1. Coupler Design and Fabrication.....	53
4.2.2. Testing.....	54
4.3. Future Work.....	54
APPENDIX.....	57
REFERENCES	61

LIST OF FIGURES

1.1: The GEM Microvascular Anastomotic Coupler from Synovis being held by its installation tool.....	4
1.2: The vascular coupling device components (inner ring on ends, outer rings in middle)	11
2.1: The outer ring and the two half couplers	14
2.2: Free body diagram of the vessel once the coupler is installed.....	17
2.3: A curve showing the relationship between the length of the inner ring cylinder and the space between the inner and outer rings	19
2.4: Previous installation tools.....	21
2.5: The installation tools. The two inner ring holders are on the left and the outer ring arm with the anvil is on the right.	23
2.6: A visual of the process of anastomosis using the vascular coupling device and installation tools. a. The two vessel ends to be anastomosed, b. snip the end of the vessel into 3 flaps of approximately 1.5 mm in length, c. secure the inner ring onto the holder, d. pass the vessel through the inner ring, e. insert the anvil into the vessel end, f. push the outer ring onto the inner ring, g. remove the outer ring arm, h. a visual of the coupler half installed, i. repeat steps a through g for the other vessel end, j. align the coupler halves so that the outer ring arms are offset 90°, k. push the coupler halves together, and l. remove the installation tools.	25
2.7: The percent leakage of the anastomosis versus the pressure of the saline flowing through. These data are for the open-end test.	33
2.8: The leak rate of saline through the anastomotic site versus the pressure of the saline. These data are for the sealed-end test.	34
2.9: Images of the tensile testing of five porcine carotid arteries anastomosed with the vascular coupling device. Failure mode 1: the artery end slipped off the hose barb connector; Failure mode 2: the inner ring slipped off the outer ring; Failure mode 3: the artery tore off the inner ring.....	38
2.10: Plot showing the force until failure of the coupled vessels	39

2.11: The outer ring installed over the inner ring on the carotid artery of a cadaver swine	43
3.1: PLA inner ring (left) and outer ring (right) fabricated using 3D printing.	46
3.2: The force of the 3D printed PLA coupler at failure.....	48
A.1: Free body diagram of the outer ring when being installed.	58
A.2: Stress concentration factor chart for a cantilevered beam with a corner [29].	59

ACKNOWLEDGEMENTS

There are many people who have helped me with this project. I would like to thank Dr. Bruce Gale for his countless hours in mentoring and advising me as well as letting me use the facilities in his lab. His council has been invaluable and timely during my years at the University of Utah. Thank you to Dr. Jay Agarwal for his instruction to me from a surgeon's point of view and for serving as a principle investigator on the project. Thanks also goes to Dr. Himanshu Sant, Dr. Jill Shea, Dr. Huizhong Li, and Brody King for their invaluable help in advising and conducting experiments. Thank you to Dr. Ken Monson and Matthew Converse for helping and letting me use their arterial tensile testing machine. Thank you to Alvin Kwok for hand suturing the cadaver vessels for the tests.

I would like to thank both the Department of Mechanical Engineering and the Department of Surgery at the University of Utah for the helpfulness of their faculty and labs.

For help in funding the project, thanks goes to the Technology Venture and Commercialization at the University of Utah, the Technology Commercialization and Innovation Program, and the Small Business Innovation Research.

Lastly, thank you to each of my family members and friends for the influence for good that they have had on my life.

CHAPTER 1

BACKGROUND

Vascular anastomosis is the connection of two blood vessels. Many surgeons frequently perform this procedure, including plastic surgeons, ENTs, vascular surgeons, cardiothoracic surgeons, and transplant surgeons. The most widely used method to perform vascular anastomosis is to hand suture the vessels together. However, the process of hand suturing is time consuming, varying on the size and location of the vessels being anastomosed, the level of experience of the surgeon, and whether the vessel is healthy or unhealthy; it leaves foreign material, the suture, inside the vessel lumen; and is susceptible to a significant amount of human error. In 2009, approximately 284 vascular operations per 100,000 population were performed in the United States [1]. Because of the large number of vascular operations that are performed, methods for improving and increasing the speed of vascular anastomosis have been researched extensively.

This project is the design and testing of a vascular coupling device aimed at improving the quality and speed of the vascular anastomosis procedure. This chapter goes over the hand suturing process, other anastomotic devices, the market potential for an anastomotic device, the prior work performed on this project, and an explanation of what this thesis covers.

1.1. **Hand Suturing**

The process of hand suturing is generally done with a needle and suture (the size of the suture depends on the size of the vessels being anastomosed), a needle driver, and forceps [2]. There are two main methods to accomplish the hand sutured anastomosis: running and interrupted. For both methods, a general process is followed. First, the surgeon will clear away the adventitia and extra fat around the ends of the vessels (about 2 to 3 mm up from the end of the vessel). This allows the anastomosis to be more secure, as the fat will not get in the way. It also will not leak as much when the anastomosis is complete. Once the extra fat is removed from the ends of the vessels, the surgeon will then drive the needle into the outside wall of vessel A, about 1 mm away from the end. They will then bring the needle to the inside wall of the other vessel end (vessel B) being anastomosed, again about 1 mm from the end. The surgeon will then take the two ends of the suture and tie them together using a square knot. The surgeon will take careful heed that the intima of vessel A is in contact with the intima of vessel B. From here, the two methods of running versus an interrupted anastomosis differ.

For a running suture, the surgeon will simply keep using the suture without cutting it, looping the suture in and out of the vessel walls using the needle driver. The suture will go from the outside of vessel A to the inside of vessel B. This continues until the surgeon has covered the circumference of the vessel. The running suture is traditionally done on larger vessels (>3 mm diameter), as it is viewed that the running suture would slightly constrict the vessel and prevent it from expanding when blood is pushed through it again.

For an interrupted suture, the surgeon will repeat the process described above in starting the hand suturing and will cut the suture after each stitch. Thus, there will be

many individual stitches around the circumference of the vessel when the anastomosis is complete. This type of suture is typically performed on smaller sized vessels as well as those vessels in which constricting the expansive properties of the vessel would be a concern. Hand suturing a vessel using the interrupted method requires a significantly large amount of time to accomplish than using the running method (about two to three times as long, depending on the vessel and the skill of the surgeon).

1.2. **Other Anastomotic Devices**

There have been many ideas put forth to accomplish vascular anastomosis using methods other than hand suturing. Among these ideas are: using a plastic ring with metal spikes [3], a stent and glue [4], staples [5], and laser welding [6].

1.2.1. GEM Microvascular Anastomotic Coupler

The most common method used for suture-less anastomosis is the GEM Microvascular Anastomotic Coupler from Synovis. This device is a plastic ring with metal spikes. The vessel end is brought through the plastic ring and the vessel wall is pulled over so that the metal spikes penetrate through the vessel wall. The process is repeated with the opposing vessel end and the two ends are then brought together. This coupler works very well with the anastomosis of veins because of the thinness and flexibility of the venous walls. However, when performing the anastomosis of arteries, the thick elastic walls of the artery tend to tear off the metal spikes, or bend the spikes, causing a misalignment. Furthermore, this coupler is not biodegradable, and thus the coupler remains in the body post-surgery. An image of this device being held by its installation tool is shown in Figure 1.1.

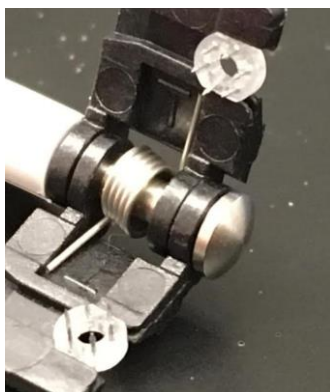


Figure 1.1: The GEM Microvascular Anastomotic Coupler from Synovis being held by its installation tool

1.2.2. Thermoreversible Intravascular Poloxamer Stent

One of the ways of using a stent and glue that is currently being tested is a poloxamer (a hydrophilic and water-soluble copolymer material) and an adhesive. A stent is a tubular structure temporarily placed inside the vessel to assist in the healing of the vessel. Once the vessels that will be anastomosed have been prepared, a liquid poloxamer is injected intraluminally. The poloxamer undergoes a phase transition into a semisolid stent upon contact with the tissue. A surgeon then applies a surgical adhesive to the circumference of the vessel end. Lastly, saline is employed to lower the local temperature, causing a reverse phase transition to liquid form. The poloxamer stent is then washed away/removed as blood flow is reestablished. Limitations with this method of anastomosis include the difficulty of handling a vessel size mismatch, the increased risk of damaging the vessel lumen, especially when the vessels are small, and its lack of data on testing a venous anastomosis.

1.2.3. AnastoClips

Using staples for vascular anastomosis is similar to using staples to close a wound in the skin. For the AnastoClips from LeMaitre Vascular, the two vessel ends to be anastomosed are prepared and brought together. Then using suture, the vessels are connected to each other at four different sites around the vessels, each 90° apart. The clips are then installed so that both of the vessel walls are pushed and held together by the clip/staple. This method of anastomosis works well for accomplishing the anastomosis rather quickly, but it does leave the metal staples implanted inside the body when the surgery is complete and is still subject to a great degree of human error.

1.2.4. Laser Welding

The laser welding involves using a 1.9 μ laser and human albumin as solder. While the time to complete the anastomosis is quicker than that of hand suturing using the running method, laser-welded anastomoses are more susceptible to pseudoaneurysm, a collection of blood that forms between the two outer layers of an artery, the muscularis and the adventitia layers. Also, the strength of the seal for the laser welded anastomosis is a concern as some seals are not able to withstand arterial pressure.

1.3. Design Research and Potential

In order to assess the potential that a vascular coupling device would have on the market and to improve the design of the coupler, surgeons performing vascular anastomosis were sought out and interviewed. Overall, 54 surgeons were interviewed, most of them being plastic and ear nose throat surgeons performing the free flap procedure (a procedure in which vascular anastomosis is performed multiple times). When interviewing the different surgeons, each person brought up aspects of the design that they liked or felt like the coupling device needed to have in order to use it. While there are still surgeons who said that they would prefer to hand suture the anastomosis over using any coupling device, a majority of the surgeons interviewed were in favor of trying a new device and they gave their input as to what they needed in the anastomotic device. While each one who was interviewed had their own desired aspects of the design that they felt the device had to have, there are common themes among these value propositions. These value propositions were taken into consideration in the design of the vascular coupling device (the work of this project). The common themes the surgeons presented are the device is able to:

- perform a quick and reliably secure anastomosis of the blood vessels
- increase the speed of the anastomosis, thus spending less time in the operating room for each case
- be intuitive in the design allowing for an easy and simple installation
- perform the anastomosis for both arteries and veins
- perform the anastomosis of an artery to a vein
- function without coming in contact with the lumen or the blood flow
- hold the vessel open
- perform an end to side anastomosis
- perform the anastomosis on damaged vessels (such as radiated or calcified vessels)

When expressing their reasons for the desired aspects of the design, it became clear why surgeons considered them as a “must have” in order to use the vascular coupling device. Depending on the case on which the surgeon (either plastic or ENT surgeon) was working, they would need to complete the anastomosis of an average of three vessels per case, one artery and two veins. Thus, they would like to use one device that would function for both types of vessels. In addition, some of the cases that these surgeons perform are time consuming. These long cases reach up to 8-10 hours in the operating room, so anything that can be done to decrease the amount of time in the OR is of a great benefit. Each anastomosis can be very time consuming, and the amount of time required to perform the hand sutured anastomosis is dependent on the skill of the surgeon and the size and exposure of the vessel. Being able to quickly perform a reliably secure anastomosis using the coupler would greatly benefit them in the surgery. Because of the

reliability of the coupler in performing a secure anastomosis, this would allow surgeons to have a peace of mind in using it, thus it would also not only physically benefit the surgeons, but emotionally as well. Another aspect of the design that surgeons viewed that the vascular coupling device must have is that it must be easy to use and install. This makes sense as surgeons would be less inclined to want to take time out of their busy schedules to learn how to use a new device. Thus, they would like the coupler to be intuitive in its design and installation.

Overall, the aspects of the design provided by the surgeons were taken into consideration and influenced the design of the vascular coupling device explained in this work as well as the future work of the project.

1.4. Prior Work

The vascular coupling device for this project was the focus of several student projects before this work was done and has undergone a few generations. An idea was originally put forth that a device should be developed that would be able to perform the anastomosis for both arteries and veins. Each newer generation improved upon previous generations. A summary of this past work follows.

1.4.1. Vascular Coupling Device with 5 Spikes on Wings that Can Rotate 45°

The first generation of the proposed device had a ring-shaped base made of polytetrafluoroethylene (PTFE) [7]. The size of the ring used is determined by the outer diameter of the vessel for which the coupling device is installed on. Stainless steel spikes are attached to the base through hinged wings and each wing is connected to the base by means of a hinge, which allows the wing to rotate 45° for proper installation of the

coupling device. The vessel being anastomosed is then pulled through the ring base, going from the side without the spikes to the side with the spikes so that the vessel end is just past the tips of the metal spikes. The spikes are then pressed through the vessel wall and rotated back 45° so that they are parallel with the vessel. The same process is performed on the other vessel end needing to be anastomosed. The two half couplers are then brought together to complete the anastomosis with the spikes penetrating from one coupler into the other from both sides. Advantages of this generation of the vascular coupling device are that there is no foreign material exposed in the blood flow and the vessel is held open, reducing the chance of blockage or collapse at the anastomotic site. A disadvantage of this is that the angled spikes do not always catch the vessels walls or the wall does not slide down the spikes as needed, requiring manual manipulation of the vessel to install the vessel wall over the spikes. The metal spikes also will not degrade and may cause problems in the body over time. Furthermore, the use of multiple materials can lead to biocompatibility concerns.

1.4.2. Second Generation of Vascular Coupling Device with 4 Spikes Rotating 90°

The second generation of the device had a plastic ring base made of PTFE or high-density polyethylene (HDPE) with four stainless steel spikes that were on hinges that were able to rotate 90° [8]. The artery would first pass through the plastic ring base about 1-2 mm past the end of the vessel. The four spikes were then driven into the vessel wall at an angle orthogonal to the vessel wall. After penetrating through the wall, the spikes then rotated on the hinges 90° so that the end of the vessel stretched and was held open. The same procedure was done on the end of the other vessel being anastomosed. These

two half couplers were then offset from each other by 45° and connected together with the spikes being inserted into the corresponding holes of the opposing half coupler. One problem with this device was this caused significant stress on the arterial walls when rotating them 90° in the four different directions. Because of the elastic nature of arteries, this stress sometimes resulted in the arterial wall tearing off the metal spike. In addition, the same potential concerns with biocompatibility exist for this device.

1.4.3. Vascular Coupling Device Without Spikes

The next generation of the vascular coupling device used a different approach in which no pins/spikes were used [9]. The device consists of two rings for each half coupler (four rings total): an inner ring and an outer ring as shown in Figure 1.2. The inner ring is made out of poly(methyl methacrylate) because of its compatibility with laser cutting. The inner ring's inner diameter is sized according to the outer diameter of the vessel being anastomosed. The inner ring is shaped like a cylinder that has a thicker base that allows it to be held by the installation tools. The vessel end is then passed through the inner ring about 3 mm. The vessel end is then clipped into three to four flaps (depending on the size of the vessel diameter) to allow for the release of tension and easier eversion of the vessel over the outer diameter of the inner ring. Once the vessel is everted over the inner ring, the outer ring is placed around the inner ring and vessel, using friction to hold the clipped ends of the vessel between the inner and outer rings. The same procedure is then done to the other vessel end being anastomosed. The two coupler halves are then brought together, the one coupler half being 90° offset from the other, and are pushed together until the arms of the outer rings clip together similar to that of a



Figure 1.2: The vascular coupling device components (inner ring on ends, outer rings in middle)

backpack clip. This device works well in creating a secure anastomosis when installed properly as well as not having any metal pins, thus the design of it allows for the coupler to be made of a biodegradable material. Concerns with this device include the overall size of the device (we would like it to be smaller), the two types of rings being made of different materials (leading to biocompatibility concerns), and the inefficiency of the installation tools when installing the coupler *in vivo*. Much of the progress made in this work is aimed to overcoming these concerns.

1.5. Thesis Overview

This thesis improves upon the work done by Cody Gehrke and Huizhong Li in Dr. Jay Agarwal's and Dr. Bruce Gale's labs. Explained in the following chapters is the design and testing of the current generation vascular coupling device and its corresponding installation tools. First, an explanation of the dimensions for both the coupler and installation tools will be provided, then the selection of materials and why those materials were chosen will be discussed. This will be followed by a description of tests that were performed along with a discussion of the results. The next chapter, supporting materials, will discuss the efforts of 3D printing, the mechanical properties of polylactic acid, and the method of sterilization to be used on the final product. Lastly, conclusions will be stated and future work on the project will be put forth.

CHAPTER 2

VASCULAR COUPLING DEVICE

The vascular coupling device to be developed and studied in this work is an effort to come up with a solution for performing a suture-less vascular anastomosis in a quick and reliable manner. Some desired benefits of the coupler include: an intima to intima contact for the anastomosis; no foreign material is in contact with the blood flow, which reduces the risk of thrombosis; the speed of completing the anastomosis, reducing the patient exposure to anesthesia, reducing the ischemic time for the tissue, and saving OR time; and a design that will be able to perform the anastomosis of both arteries and veins. This chapter discusses the design, testing, and analysis of results of the revised vascular coupling device with its installation tools.

2.1. Design of the Vascular Coupling Device

The current vascular coupling device is very similar to the most recent generation of the device described in the previous chapter (see section 1.4.3.). Each half of the coupler consists of two parts (Figure 1.1). The first part is an inner ring that is shaped like a cylinder, with one end of the cylinder having a “plate” with a hole attached to it. This “plate” acts as a base by which the inner ring holder of the installations tools is able to grab and hold onto the inner ring while providing a platform for the arms of the outer ring to grasp. The next part is an outer ring (see Figure 2.1) that has two arms coming off it on

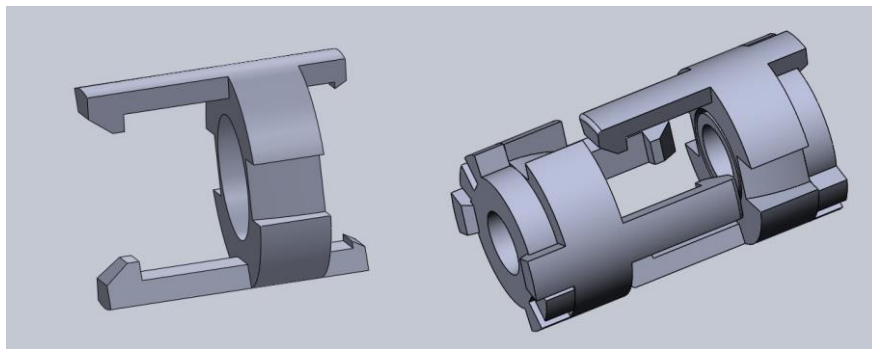


Figure 2.1: The outer ring and the two half couplers

each side. At one end, the arms are shorter in length (2 mm). These arms will grab onto the base of the inner ring. The other arms are longer in length (6 mm) as they grab onto both the opposite outer ring and inner ring. On the outside diameter of the ring on the outer ring are two grooves that are mirrored from each other across the center of the ring. These grooves are for the long arms of the opposite outer ring. The long arms will pass through the grooves and hold onto the base of the opposing inner ring. Figure 2.1 shows two half couplers with the outer rings aligned with each other so that the long arms will pass through the grooves of the opposing outer ring.

2.1.1. Justification of Length of Inner Ring Wall/Spacing

Between Inner and Outer Rings

Because the coupler will be implanted in the body, it is beneficial to have the coupler as small as possible and still function correctly. Thus, calculations were made to determine two critical dimensions in the design of the coupler: the length of the inner ring wall (the part shaped like a cylinder) and the spacing between the inner and outer rings. Each vessel that is anastomosed is different in diameter, wall thickness, and age, and thus the mechanics of each vessel will differ. Therefore, these calculations are considered to be examples and not exact dimensions.

To help determine the force necessary to hold the vessel in place once the coupler is installed, Newton's second law that the sum of the forces acting on an object is equal to the product of the mass and acceleration of the object is considered. Physiologically, the two main forces acting on the vessel are the axial tensile force and the frictional force between the vessel and the coupler, resulting from the vessel wall being held in place by the inner and outer rings. The vessel being everted is treated as an ideal frictionless

pulley. This pulley assumption is a conservative approach, and it is noted that in actuality, the force generated by the coupler will be larger than is accounted for in these calculations. Using the pulley assumption, the frictional force must be equal to the axial tensile force for the coupler to hold the anastomosis intact. See Figure 2.2 for the free body diagram of the blood vessel. Note that blood pressure is involved as contributing to the axial tensile force that the vessel experiences as it causes a longitudinal stress in the vessel wall [10].

To calculate the length of the inner ring cylinder and the spacing between the inner and outer rings, the assumptions are made that the blood vessel wall is incompressible and that the vessel can be considered to be a thin walled cylindrical pressure vessel. This allows us to calculate the stresses in the vessel wall. First, the longitudinal stress σ_z is given by the equation for a thin walled cylindrical pressure vessel:

$$\sigma_z = \frac{Pr}{2t} \quad (\text{Equation 2.1})$$

where P is the physiological pressure, r is the radius of the vessel, and t is the thickness of the vessel wall. The assumption that the vessel is incompressible gives the relation $\lambda_r \lambda_\theta \lambda_z = 1$, where λ_r is the stretch ratio in the radial direction, λ_θ is the stretch ratio in the circumferential direction, and λ_z is the stretch ratio in the longitudinal direction. By using the definitions of the stretch ratios in the radial and circumferential directions the incompressibility relation can be described as:

$$\lambda_z \frac{2\pi r_f t_f}{C_o t_o} = 1 \quad (\text{Equation 2.2})$$

where r_f is the final radius of the vessel, C_o is the initial circumference of the vessel, and t_f and t_o are the final and initial thicknesses of the vessel wall, respectively. The longitudinal stress can then be related to the relevant Kirchhoff stress S_z using the stretch

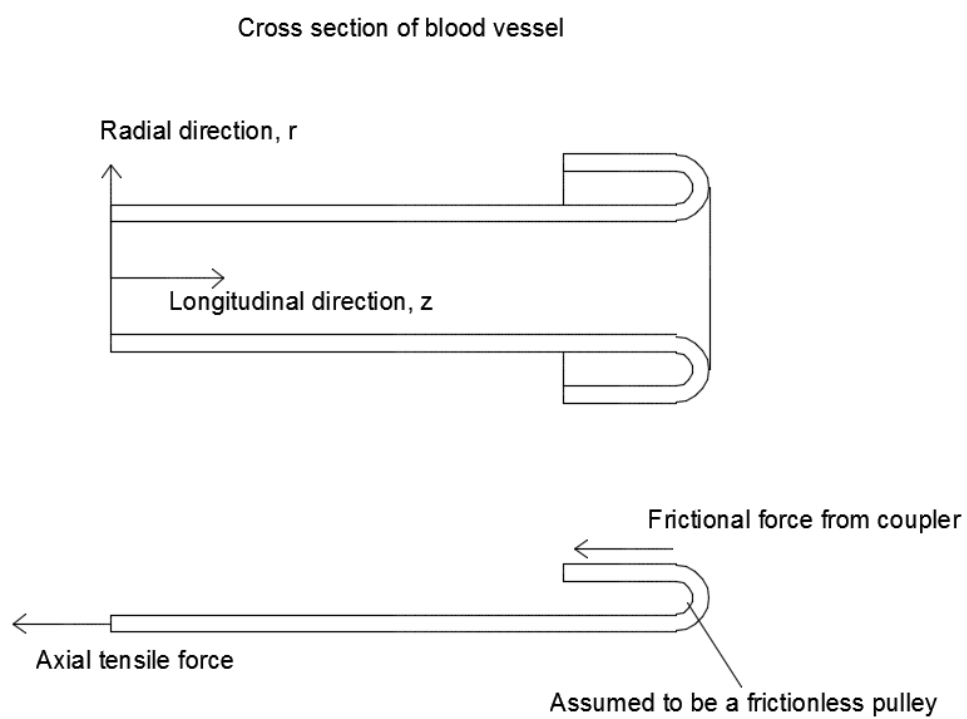


Figure 2.2: Free body diagram of the vessel once the coupler is installed

ratios λ [11] [12]:

$$\sigma_z = \lambda_z^2 S_z \quad (\text{Equation 2.3})$$

Combining equations 1-3 and the assumption that the change in radius is minimal, the Kirchhoff stress due to physiological conditions is approximately:

$$S_z = \frac{Pr t_f}{2t_o^2} \quad (\text{Equation 2.4})$$

A similar process is followed for the Kirchhoff stress due to the coupler. However, this time, the longitudinal stretch ratio λ_z can be related to the ratio of the length of the inner ring cylinder L and the length of the flap cut into the end of the vessel L_{flap} . The resulting stress value is:

$$S_z = \frac{NL_{flap}^2}{4\pi t_f L^3} \quad (\text{Equation 2.5})$$

where N is the normal force acting on the vessel from the coupler. Due to the balance of forces, the stresses in equations 4 and 5 are divided by the areas and can be set equal to each other. This is then solved for the minimum length of the inner ring cylinder L :

$$L = \left[\frac{2NL_{flap}^2(r_f + t_f)}{4\pi P r_o(r_o + t_o)} \right]^{1/3} \quad (\text{Equation 2.6})$$

In calculating the normal force, the frictional force is employed using the relation $F_{friction} = \mu N$, where μ is the coefficient of friction. Under extreme conditions with a blood pressure of 225 mmHg and 20% elongation, the axial stress is approximately 112 kPa, corresponding to an axial force of 1.4 N [13]. The coefficient of friction between a blood vessel and a catheter has been determined experimentally to be about 0.08 [14]. By varying the value of the spacing between the inner and outer rings, a range of lengths for the cylinder of the inner ring can be determined. Graphically shown in Figure 2.3 is the curve of the length of the inner ring cylinder versus the space between the inner and outer

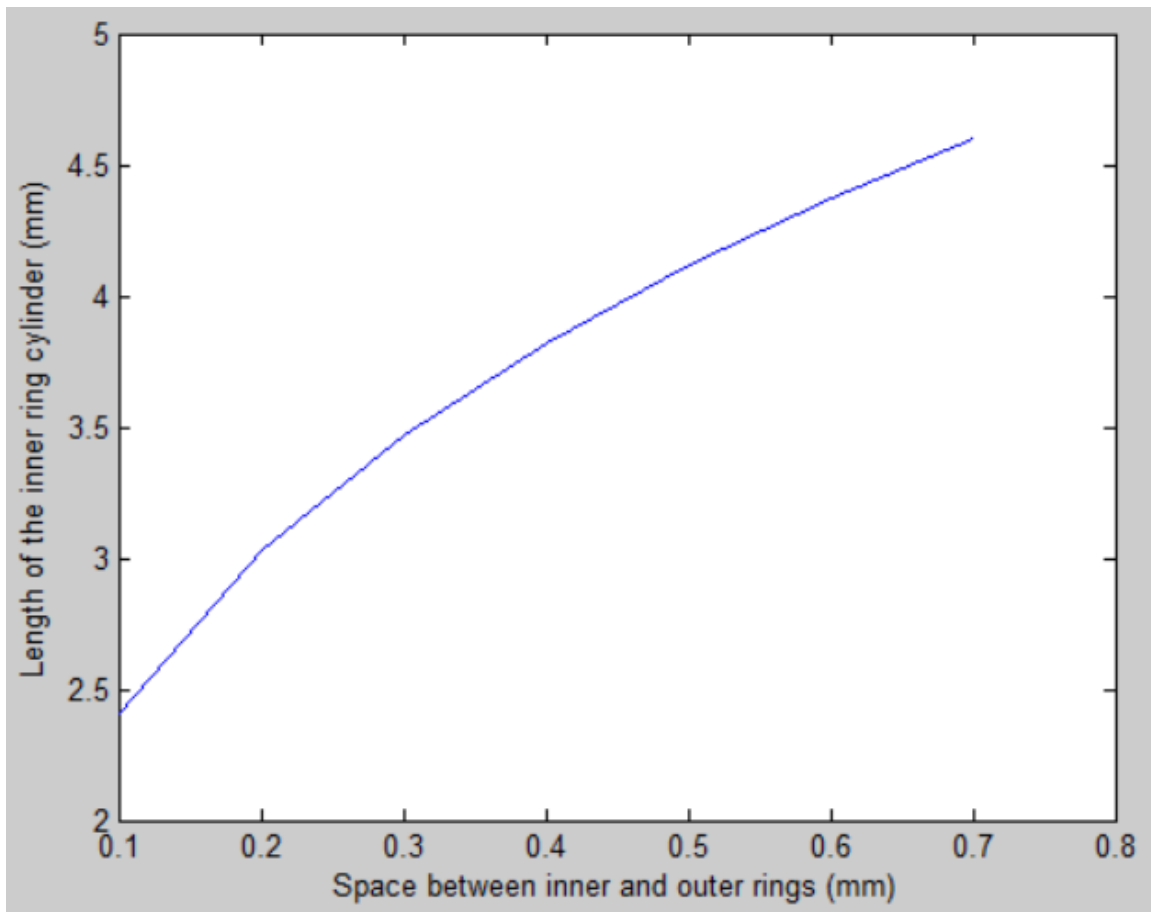


Figure 2.3: A curve showing the relationship between the length of the inner ring cylinder and the space between the inner and outer rings

rings. It can be determined that generally, the cylinder of the inner ring should have a length of approximately 3 mm and the spacing between the inner and outer rings should be about 0.2 mm, although these values will change depending on the vessel being anastomosed. Furthermore, it must be remembered that these results are approximations because of the assumptions that the vessel is incompressible and it can be considered to be a cylindrical pressure vessel.

2.2. Design of the Installation Tools

The current installation tools for the vascular coupling device were developed using certain successful features of the previous installation tools and making necessary improvements upon other features.

2.2.1. Previous Installation Tools

The previous installation tools designed and fabricated to facilitate the installation of the vascular coupling device consisted of a holder and an anvil instrument and are shown in Figure 2.4 [9]. The holder was used for holding the inner ring. The holders had a pinned connection at the end opposite of where it held the inner ring. There was one holder used for each end of the vessel being anastomosed. The heads of the two holders were offset by 90°, allowing the two half couplers to be properly aligned when completing the anastomosis. The anvil instrument was used to hold the outer ring by means of an anvil head. The anvil head was designed to plunge into the vessel and evert the clipped vessel end. The instrument then pushed the outer ring onto the inner ring, holding the vessel open by holding the clipped vessel end between the inner and outer rings using a friction fit. Both tools were fabricated from acrylonitrile butadiene styrene (ABS) and Vero White by means of 3D printing.

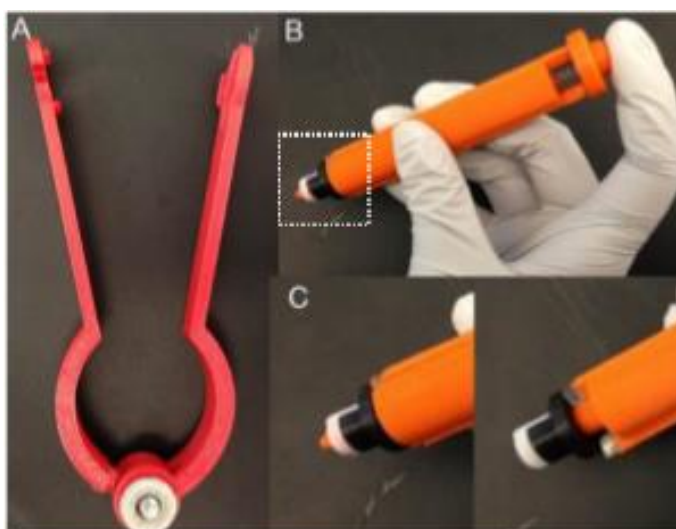


Figure 2.4: Previous installation tools

The installation tools proved to perform well on benchtop experiments. The installation tools were tested on cadaver arteries, veins, and expanded polytetrafluoroethylene (ePTFE) tubing. However, some struggles with the installation tools occurred when using them in an animal study. It was difficult for the surgeon to use the instruments inside the incision wound because of the large size of the instruments. In addition, in order to install the outer ring, the anvil instrument needed to be perpendicular to the holder instrument. Due to the limited space inside the incision wound, this process was difficult to perform without the vessel slipping back out of the inner ring before the outer ring could be installed.

2.2.2. Modified Installation Tools

The installation tools developed in this work for the vascular coupling device consist of two main parts: an inner ring holder and an outer ring arm (Figure 2.5).

The inner ring holder is designed to be similar to forceps commonly used by surgeons. It was designed this way in order to significantly decrease the bulkiness of the tools and to increase the ease of use for surgeons, as they are familiar with how to use forceps in surgeries, thus increasing the ease of installation of the vascular coupling device. At the tip of the inner ring holder, the points have a small back plate and notch to grab onto the inner ring to be able to hold the inner ring in place while pressure is applied to install the coupler. Because of this forceps-like design, the inner ring holder is able to adjust to the different sizes of inner rings and can function for each of them; thus, the same tool will work for different vessel sizes. The inner ring holder is able to connect to the outer ring arm at the top by means of a pinned connection. The outer ring arm is a bar with a platform and anvil on the end opposite of the pinned connection. The platform is



Figure 2.5: The installation tools. The two inner ring holders are on the left and the outer ring arm with the anvil is on the right.

designed to hold the outer ring by means of the long arms of the outer ring. The platform is able to hold the different sizes of the outer ring. The anvil is designed so that the end of it will plunge into the lumen of the vessel and pin the vessel wall against the inside wall of the inner ring, preventing the vessel from slipping away. The anvil will also evert the vessel enough that when the outer ring is installed, it will fully evert the vessel. The outer ring is placed upon the platform so that the short arms of the outer ring are facing the inner ring, and when the outer ring arm swings down, the anvil will evert the vessel and the outer ring will be pushed upon the inner ring, holding the vessel open. At this point, the outer ring arm is removed from the outer ring and the inner ring holder is left attached to the coupler. A similar process is done to the other end of the vessel. Once the two halves of the coupler are installed, the two inner ring holders are pushed together, causing the two halves of the coupler to come and “clip” together. The two inner ring holders are then removed from the coupler and the anastomosis is complete. Figure 2.6 shows a series of images of the anastomosis procedure just described.

2.3. Selection of Materials

2.3.1. Materials of the Coupler

One of the goals of the vascular coupling device is to leave no foreign material implanted in the body for a prolonged period of time. Therefore, much research has been done on biodegradable materials that are able to hold their structure when fabricated into the shapes of the vascular coupling device and will not have any detrimental effects when implanted *in vivo*. Research on one biodegradable material (polylactic acid) is explained more in depth in Chapter 3. However, in order to obtain a proof of concept that the coupler will function properly as designed, less expensive non-biodegradable materials

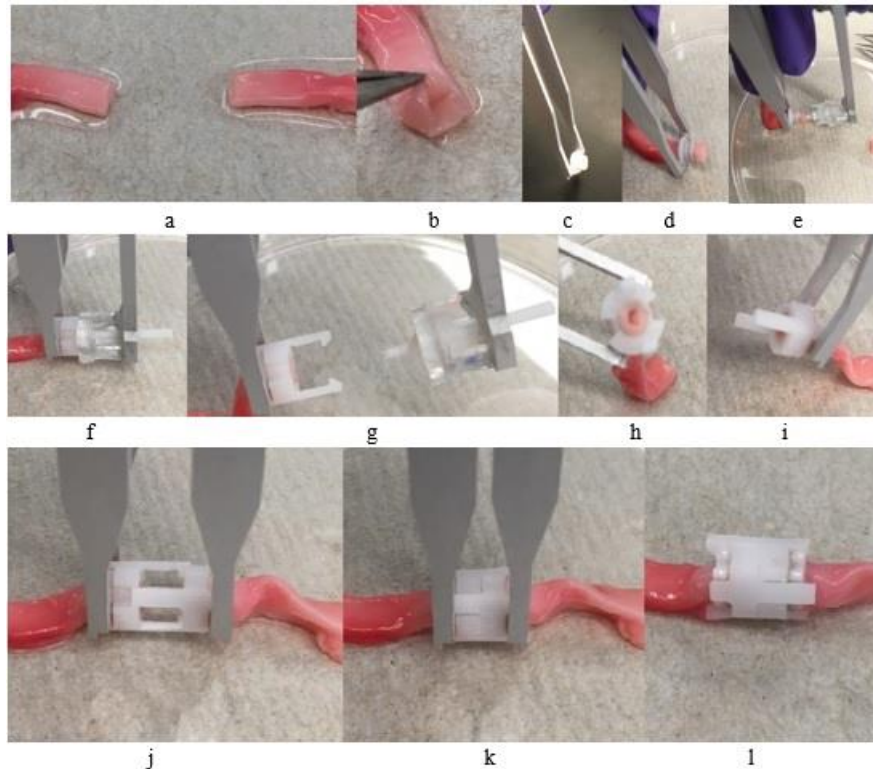


Figure 2.6: A visual of the process of anastomosis using the vascular coupling device and installation tools. a. The two vessel ends to be anastomosed, b. snip the end of the vessel into 3 flaps of approximately 1.5 mm in length, c. secure the inner ring onto the holder, d. pass the vessel through the inner ring, e. insert the anvil into the vessel end, f. push the outer ring onto the inner ring, g. remove the outer ring arm, h. a visual of the coupler half installed, i. repeat steps a through g for the other vessel end, j. align the coupler halves so that the outer ring arms are offset 90° , k. push the coupler halves together, and l. remove the installation tools.

were used.

The materials used for the vascular coupling device were selected with two main purposes in mind: 1) the material must be biocompatible, and 2) the material must be able to maintain its structure when fabricated, especially when the parts are so small. With these two main purposes in mind, other aspects also influenced the determination of which materials to use such as ease of manufacturing and low cost. The inner ring is constructed out of poly(methyl methacrylate) (PMMA) because of its compatibility with laser cutting. Using a PMMA sheet, a CO₂ laser cuts two rings (for the cylinder of the inner ring) and a base. The two rings and base are then glued together using cyanoacrylate glue. Both PMMA and the cyanoacrylate glue are biocompatible and do not cause any inflammatory reactions when implanted in body tissue [15].

The outer ring is machined out of high-density polyethylene (HDPE). HDPE was chosen because of its biocompatibility and it is also able to hold its structure when machined into a small part. HDPE is also less brittle than PMMA, and thus the outer ring arms do not snap off when fully installing the coupler. Eventually, both the inner and outer rings will be manufactured from a biodegradable material. One material in particular that has been looked into is poly-L/D-lactide, whose properties are discussed more in Chapter 3.

2.3.2. Materials of the Installation Tools

The materials of the installation tools were selected based on the needs of the design as well as convenience of manufacturing. The previous installation tools were fabricated of ABS. While it was extremely convenient to manufacture them as they were simply 3D printed, this presented a problem. The installation tools experience a significant amount

of stress when installing the coupler and thus the thickness of the installation tools needed to be increased to avoid fracture. However, because of the bulkiness of the instruments, it was difficult to install the coupler in areas of limited accessibility. Thus, for the current installation tools, a metallic material was selected as it would have the strength necessary to install the coupler without failure and be able to be small as well. The material selected for the prototype of the installation tools, specifically the inner ring holder and the outer ring arm, was aluminum 7075-T651. This material was selected because the aluminum provided the needed strength for the instruments to install the vascular coupling device as well as a lower price when compared to other metals. Once the design of the tools is verified, the desired material is a surgical stainless steel as it has a higher stiffness and will fatigue much slower than the cheaper aluminum. Note that the installation tools are designed in such a way that they could be used multiple times or be disposable if a mold were made and parts were metal injection molded.

The material selected for the anvil was Vero White, which was chosen because it is biocompatible and can be fabricated quickly using 3D printing. This 3D printer used a stereolithography apparatus (SLA) method to print. This method cures segments of a pool of resin to create the 3D printed object. Wrapped around the head of the anvil is PTFE tape to decrease the friction, thus preventing the vessel from sticking to the anvil during the vascular coupling device installation process.

2.4. Testing Protocol

In order to prove the functionality of the vascular coupling device, a series of tests on the coupler and installation tools were implemented. For these tests, cadaver vessels (porcine carotid arteries) were used and both coupled vessels with the vascular coupling

device and hand sutured vessels by a microsurgeon were tested and compared to each other. Porcine carotid arteries were selected because of the minimal number of branches the vessels have. The benchtop tests that were performed were two types of leak tests (an open-end pressure test and a sealed-end pressure test), a tensile test, and a test measuring the time to complete the anastomosis.

2.4.1. Leak Tests

Two different types of leak tests were performed on the vascular coupling device: an open-end pressure test and a sealed-end pressure test. The open-end pressure test was performed to analyze how the coupled vessels were able to allow flow through it in terms of percent leakage and compare to that of the sutured vessels. The sealed-end pressure test was performed to analyze the coupled vessels' capability to withstand pressure in terms of a leak rate and compare it to that of the sutured vessels.

An open-end pressure test was performed on both the coupled and hand sutured cadaver vessels (porcine carotid arteries). Three coupled and three hand sutured vessels were tested. One end of the vessel (away from the anastomotic site) was connected to a reservoir of saline (99.1% H₂O, 0.9% NaCl) and the other end drained into a beaker. Saline was used as a substitute to blood as it does not cause the cadaver vessel to swell or shrivel. The reservoir of saline was pressurized to three different pressures (160, 260, and 360 mmHg) and 40 mL of saline was pushed through the vessel. The pressure values were chosen to test against the higher end of blood pressures that would occur in the human body. Once the 40 mL of saline left the pressurized chamber, the amount of saline collected in the beaker was measured. It was determined that the difference between the original 40 mL and the amount collected in the beaker was lost due to leakage in the

anastomotic site. The open-end pressure test was performed three times for each vessel for each pressure for both constant pressure and pulsating pressure to mimic a heartbeat.

A sealed-end pressure test was also performed on both the coupled and hand sutured cadaver vessels. The set up for the sealed-end test was similar to that of the open-end pressure test. One end of the vessel (away from the anastomotic site) was connected to a reservoir of saline (99.1% H₂O, 0.9% NaCl) and the other end was sealed off. The reservoir of saline was pressurized to three different pressures (160, 260, and 360 mmHg) corresponding to the higher end of blood pressures in the human body. The pressurized saline was pushed into the cadaver vessels for a certain amount of time and the amount of saline that leaked was collected and measured. The leak rate was then calculated. The sealed-end pressure test was performed three times for each vessel for each pressure for both constant pressure and pulsating pressure.

2.4.2. Tensile Test

The ability of the vascular coupling device to resist tensile stress was tested and determined using a uniaxial tensile test until failure for five porcine carotid arteries. For a control, three hand sutured porcine carotid arteries also underwent the same test. To mount the vessels to the testing machine, both ends (away from the anastomotic site) were fit around a 1/16 inch hose barb and were tied down using 3-0 silk suture and cyanoacrylate glue. The hose barbs and the associated fixtures were then attached to a custom vertical linear stage (Parker Automation, Cleveland, OH). The superior fixture was attached to an X-Y stage (MS-125-XY, Newport, Irvine, CA) that allows for correction of any barb misalignment. The X-Y stage was suspended from a 10 lbs capacity load cell (Model MDB-10, Transducer Techniques, Temecula, CA). The inferior

fixture was attached directly to the stage. Digital encoders having a resolution of 1.0 μm gave the linear stage positions. To implement the tensile stress in the vessel, the stage translated both fixtures at equal velocities in opposite directions. This allowed the anastomotic site to remain relatively stationary in place during the test. Images of the vessels were captured by means of a digital video camera (PL-A641, Pixelink, Ottawa, Canada) equipped with a zoom lens (VZM450i, Edmund Optics, Barrington, NJ). The test data and video were obtained by using a custom LabVIEW program (National Instruments, Austin, TX). The hydration of the vessels was accomplished by using phosphate buffered saline (Gibco PBS (10X) pH 7.4, Thermo Fisher Scientific, Salt Lake City, UT). The vessels were kept hydrated until mounting to the testing machine, after which they were immediately pulled axially from a buckled configuration until failure.

2.4.3. Time for Anastomosis

Following the procedure described above in section 2.2.2. and as shown in Figure 2.6, the time required to complete the anastomosis was measured for installing the coupler on cadaver arteries. This test was performed *ex vivo* in a confined space simulating the incision opening in an actual surgery. The timer started at the beginning of the first step of anastomosis using the installation tools, when snipping the vessel ends to create the flaps for eversion of the vessel. The timer stopped when the two halves of the coupler were brought and clipped together. To also help determine the ease of installation, a student engineer who was inexperienced with the vascular coupling device performed the anastomoses for the timed test after initially being shown how to execute the procedure. To compare with hand suturing, the time was also measured for how long it took a microsurgeon to perform a hand sutured anastomosis on cadaver vessels,

beginning when the surgeon pushed the needle through the vessel wall for the first stitch and ending when the last stitch was tied.

2.5. Testing Results and Discussion

2.5.1. Leak Tests Results and Discussion

The types of anastomoses performed and used in the leak tests are summarized in Table 2.1 (i.e., which size couplers were used as well as the suture size and hand suturing method).

The open-end leak tests reported the amount of saline that leaked from the coupled/hand sutured anastomotic site. The data shown in Figure 2.7 graphically report the percent leakage for each anastomosis.

The sealed-end leak test reported the leak rate that leaked from the coupler/hand suture anastomotic site. The data shown in Figure 2.8 graphically report the leak rate versus the pressure at which the anastomosis leaked.

It can be seen in general that the hand sutured vessels leaked more than those that were anastomosed by means of the vascular coupling device. To compare these results statistically, a two-sample *t*-test was employed to determine the difference of the leak rates. The *t*-test shows that at the higher pressure of 360 mmHg, the leak rates between the vascular coupling device and hand sutured anastomosis are statistically different ($p = 0.003$) and close to being statistically different ($p = 0.065$), assuming a confidence level of 95%, at the lower pressure of 160 mmHg. This indicates that as the pressure increases, the vascular coupling device will perform better than the hand sutured vessels in that it will leak less. When this test was performed, three of the coupled vessels formed holes in the walls of the vessels away from the anastomotic site. When saline was pressurized and

Table 2.1

Types of anastomosis performed for the anastomoses tested

Anastomosis Type	Notes
Coupler 1	Sized for 4mm diameter vessel
Coupler 2	Sized for 5mm diameter vessel
Coupler 3	Sized for 3mm diameter vessel
Coupler 4	Sized for 3mm diameter vessel
Suture 1	6-0 prolene suture, running
Suture 2	9-0 nylon suture, interrupted
Suture 3	6-0 prolene suture, running

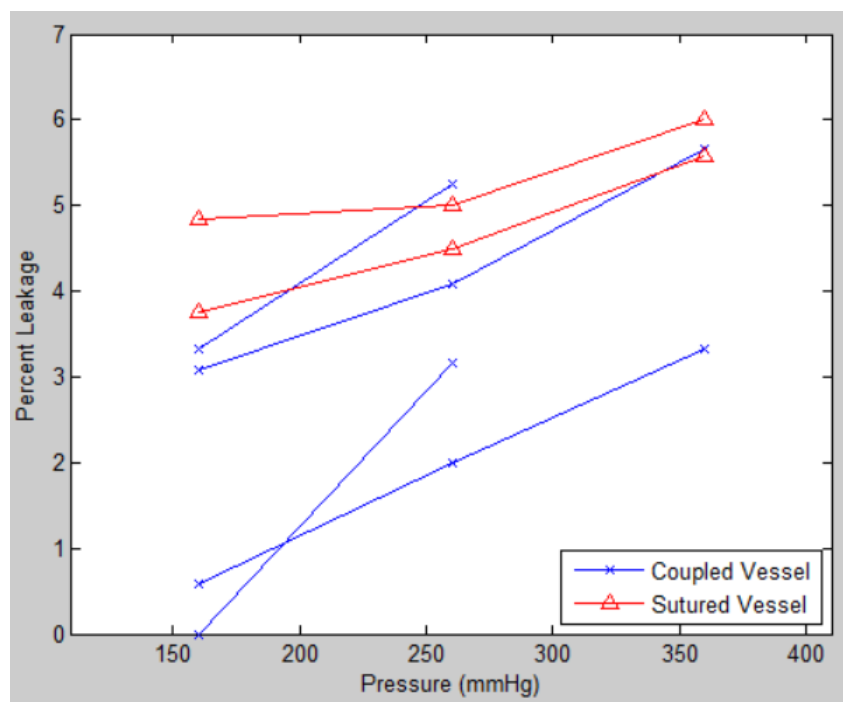


Figure 2.7: The percent leakage of the anastomosis versus the pressure of the saline flowing through. These data are for the open-end test.

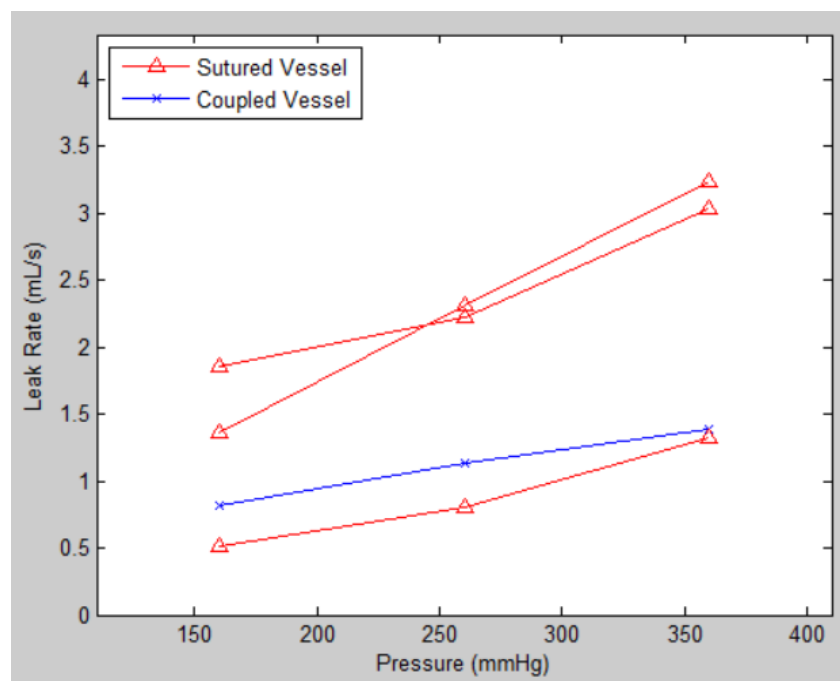


Figure 2.8: The leak rate of saline through the anastomotic site versus the pressure of the saline. These data are for the sealed-end test.

pushed through the vessels, there was no noticeable leakage originating from the anastomotic site, showing that the vessel failed in a different spot before it failed at the anastomotic site or areas immediately surrounding the coupler. Other vessels ($n = 5$) were also coupled and tested; however, a similar occurrence happened in that the vessel walls formed holes before the anastomotic site indicated any leakage. This occurrence seems to indicate that the vessel will fail in different areas before it will fail at the coupled anastomotic site. Something of note is that in Figure 2.8, the leak rates for two of the sutured vessels are relatively the same (values of about 3 mL/s for a pressure of 360 mmHg). These two sutures were accomplished using the running method with size 6-0 suture. The leak rates for the one coupled vessel and other sutured vessel are similar as well. This suture was accomplished using the interrupted method with size 9-0 suture. These results show that the coupler could be used in actual surgeries without concern of having too much leakage from the anastomosis, as both running and interrupted sutures are performed in surgeries today.

In Figure 2.7, the anastomoses that were performed by means of the vascular coupling device in general leaked less than those that were hand sutured. A few of the couplers did not have any leakage. Statistically, a two-sample t -test was run comparing the percent leakage of the coupled vessels to that of the hand sutured vessels. Based on the results of the t -test, the percent leakage of the coupled vessels and hand sutured vessels is statistically different ($p = 0.0002$) at the lower pressure tested (160 mmHg) and close to being statistically different ($p = 0.061$) at the higher pressure (360 mmHg). Thus at the lower pressure, the vascular coupling device will outperform the hand sutured anastomoses in having a lower percent leakage. One thing of note is that one of the

coupled vessels had a similar percent leakage to those of the hand sutured anastomoses. This coupler was installed with a coupler sized for a 3 mm outer diameter vessel. The vessel, however, was approximately 3.5 mm in diameter, and thus the vessel was “crimped” a little bit. Therefore, when the two coupler halves came together to complete the anastomosis, the two cross sections were not completely circular, and thus it was expected that this anastomosis would leak more than the other coupled vessels. This occurrence helps explain why at the higher pressure, the two types of anastomosis perform the same. However, even with this deficiency, the anastomosis still performed similarly to the hand sutured vessels for the open-end leak test and better than the running sutures for the sealed-end leak test. These results suggest that the size of the coupler relative to the vessel size is very important in the successful use of the coupler and that 0.5 mm differences are significant enough to cause additional leakage.

When the cadaver vessels were connected to the pressurized reservoir of saline for the sealed-end pressure test, it was noticed that the vessels appreciably expanded to approximately twice their regular size. The anastomotic sites for the coupled vessels were constrained, so those areas remained the same size while those of the sutured vessels did expand. For the coupled vessels, the anastomotic site remains relatively stationary, allowing for a quick healing of the vessel lumen. Ideally, for a biodegradable coupler, the vessel will heal while being held in place by the coupler, and then the coupler will degrade away, once again allowing the vessel to expand and contract as needed.

2.5.2. Tensile Test Results and Discussion

The tensile test instrumentation reported the force at failure and the failure type for each anastomosis was observed. A series of photographs showing examples of the

various failure modes when performing the tensile test for the coupler anastomosis is shown in Figure 2.9. The average value for the axial force at failure for the vascular coupling devices is 5.52 ± 2.19 N. The curves showing the force until failure for the vascular coupling devices is shown in Figure 2.10. For normal physiological loading (a blood pressure of 100 mmHg), the axial stress on the vessel walls is approximately 13 kPa at 0% elongation and 50 kPa at 20% elongation [13] [16]. This stress corresponds to 0.64 N for a 3 mm inner diameter blood vessel. Under extreme conditions with a blood pressure of 225 mmHg and 20% elongation, the axial stress is approximately 112 kPa, corresponding to an axial force of 1.4 N [13]. Even under these extreme conditions, the vascular coupling device is able to withstand and hold the anastomosis with a factor of safety of 3.94 for extreme conditions and 8.62 for normal conditions. For comparison, the average value for the axial force at failure for the hand sutured vessels is 5.90 ± 3.09 N.

Of the five coupled vessels tested, only one of them failed by means of the inner ring slipping out of the outer ring (see Figure 2.9d). Most of the vessels failed by the vessel slipping out of the space between the inner and outer rings. When future anastomoses are performed using the coupler, consideration will go into increasing the eversion distance of the vessel over the inner ring as well as decreasing the space between the inner and outer rings as this would decrease the probability of the coupler failing by the vessel slipping out of the space between the inner and outer rings. One thing of note is that as shown in Figure 2.10, vessel 4 partially failed and then recovered and resisted a larger force than before when it partially failed. This phenomenon was caused by the extra adventitial layer on the outside of the vessel first losing a hold of the outside of the coupler (see the middle image of Figure 2.9d). The adventitial layer was held to the coupler by

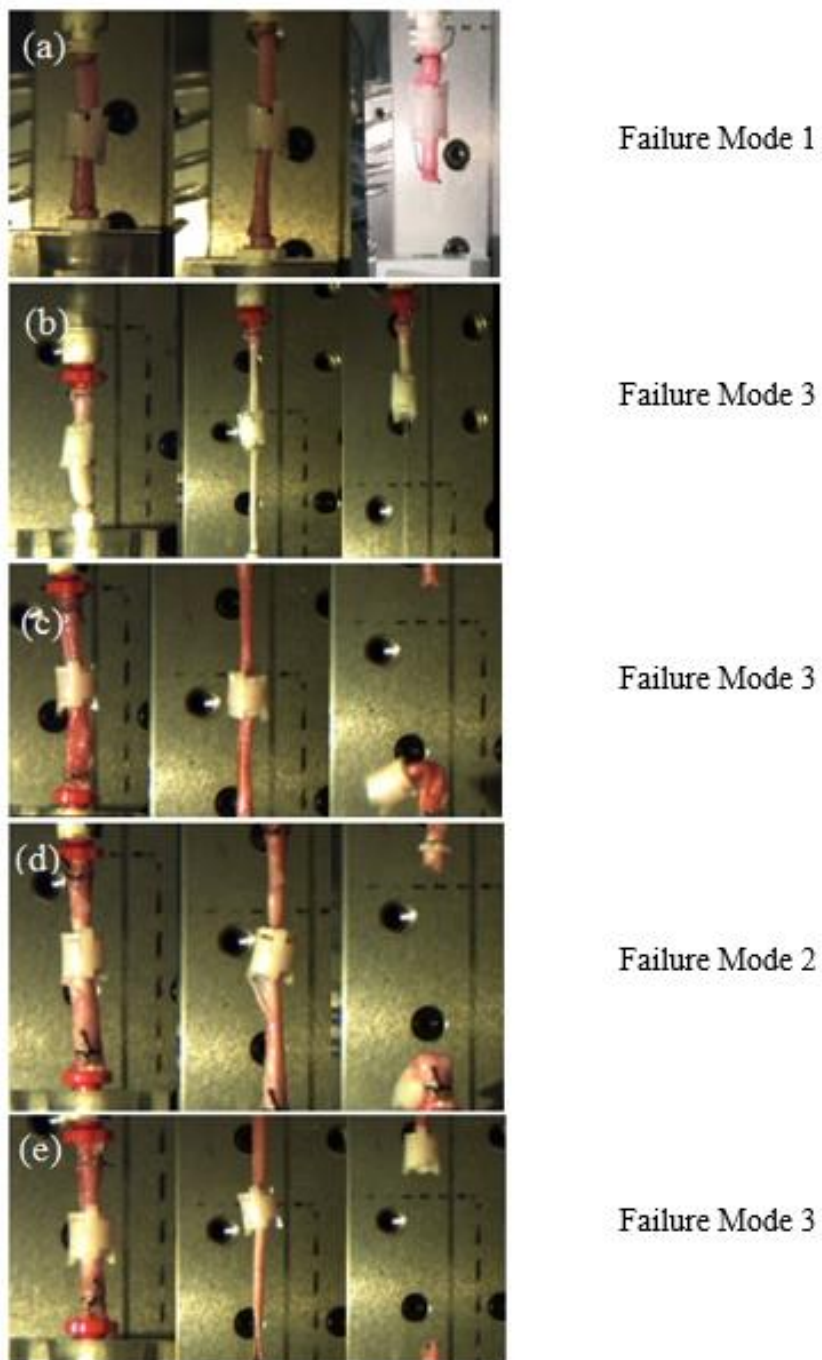


Figure 2.9: Images of the tensile testing of five porcine carotid arteries anastomosed with the vascular coupling device. Failure mode 1: the artery end slipped off the hose barb connector; Failure mode 2: the inner ring slipped off the outer ring; Failure mode 3: the artery tore off the inner ring.

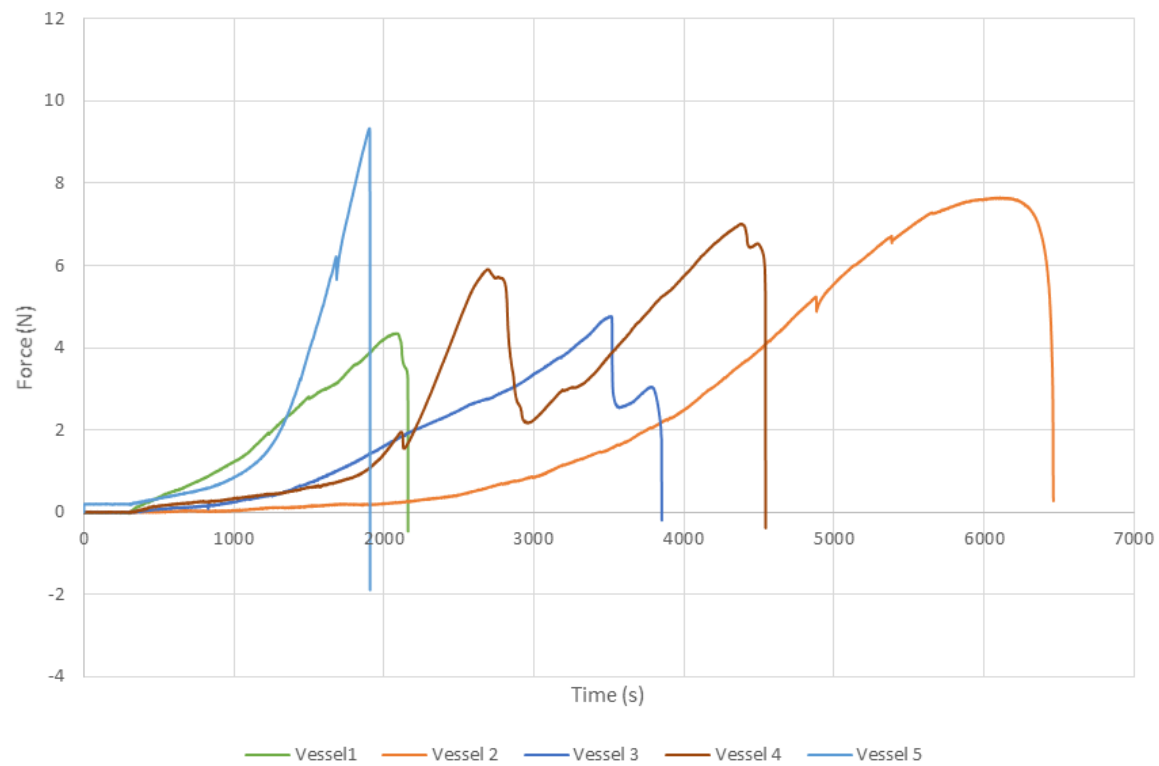


Figure 2.10: Plot showing the force until failure of the coupled vessels

means of friction. This showed that the friction between the vessel and the coupler in areas that are not between the inner and outer rings does have the potential to resist a tensile load.

2.5.3. Time for Anastomosis Results and Discussion

The time to complete the anastomosis for both the vascular coupling device and hand suturing is shown in Table 2.2. The time required to complete the anastomosis using the vascular coupling device took on average under 10 minutes to complete (the average time being 7 minutes and 34.3 seconds), with one of the anastomoses taking under 5 minutes. It is noted that the anastomoses were performed by a student engineer who was inexperienced with the coupling device. After initially shown how to perform the anastomosis, the student engineer performed these timed anastomoses. Once experienced with how to perform the anastomosis using the coupler and installations tools, the anastomoses is easily performed in under 5 minutes. The time required for the hand sutured vessels varied significantly, depending on the hand suturing method. The running suture took under 10 minutes to complete the anastomosis, but the interrupted suture took over 30 minutes to complete. The hand suturing of the vessels was performed on a benchtop with the assistance of a microscope. In actual surgeries, microsurgeons use the interrupted method more often than not to complete the anastomosis, as the running suture tends to constrict the anastomotic site. Also, the surgeon in most cases will not have the benefit of a large amount of space to work in, with the vessels sometimes being located in areas of limited accessibility. Therefore, when used, the vascular coupling device will be able to save microsurgeons a substantial amount of time in the operating room.

Table 2.2

Data showing the time required to complete the anastomosis.

Anastomosis Type	Time (min:sec)	Notes
Coupler 4 mm	4:27	
Coupler 5 mm	10:15	
Coupler 3 mm	8:01	
Running Suture	7:10	6-0 Prolene Suture
Running Suture	7:41	6-0 Prolene Suture
Interrupted Suture	34:20	9-0 Nylon Suture

2.6. Cadaver Animal Study

One of the main aspects of the vascular coupling device desired by the surgeons interviewed is the ease of use when installing the coupler. A cadaver animal study was implemented to determine the ease of installation in a mock surgery scenario. Using both of the carotid arteries on a cadaver swine (approximately 45 kg), the coupler was installed twice, once per artery. After cutting the carotid artery, the vessel end was inspected visually and it was determined what size coupler to use based on the vessel diameter and wall thickness. The size of the coupler used in this study was for vessels of 3.0 mm outer diameter. The outer ring was then installed over both the inner ring and vessel end using the installation tools with minimal difficulty. The most difficult part of the procedure was pulling the vessel end through the inner ring. Using the correctly sized anvil (based on the coupler size used, the size used in this study being for a 3.0 mm outer diameter vessel), the anvil pinned the vessel against the inside of the inner ring so that when the outer ring was installed, the vessel did not slide away through the back end of the inner ring. Shown in Figure 2.11 is an image of the outer ring installed over the inner ring. As can be seen, the vessel end is held open so that when connected to the other half coupler, the risk of collapse of the vessel and thrombosis occurring is reduced when the blood flow is reestablished. Something of note during the surgery is when the carotid artery was cut, the vessel retracted bidirectionally due to the natural tension in the vessel so that there was approximately a two and a half inch gap between the two vessel ends. This gap is also increased when installing the coupler as both vessel ends are everted approximately two millimeters on both sides. To accommodate for this extra gap, an ePTFE tube graft of similar diameter to the vessel was used and connected by means of

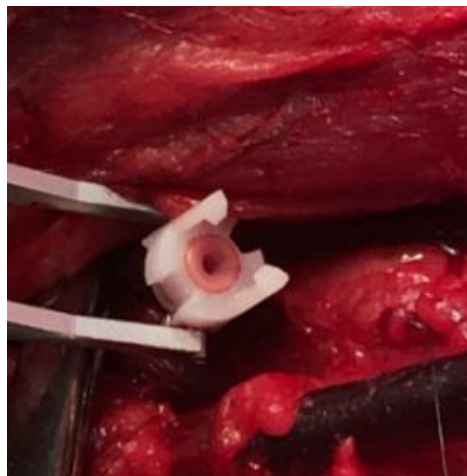


Figure 2.11: The outer ring installed over the inner ring on the carotid artery of a cadaver swine.

the coupler. The expanded polymer has been used for vascular grafts for over forty years, and ePTFE was selected because it is biostable, does not deteriorate within the body, and its reaction with blood components is minimized because the surface of the graft is electronegative [17].

The cadaver animal study confirmed the ease of use of the installation tools when installing the coupler. The carotid artery is deep in the animal and the installation tools were able to function in the more difficult exposure. The coupler is easy to install when the inner ring, outer ring, and the anvil are the appropriate size for the vessel being anastomosed. One problem that had been experienced before when installing the outer ring was the vessel would slide out of the inner ring instead of being everted by the anvil. This slide out of the vessel was caused by the anvil being too large in that the tip of the anvil was less likely to penetrate into the inside of the vessel but would instead hit the wall and push the vessel back as it entered. However, with the anvil being the correct size, the tip of the anvil entered the inside of the vessel, pinning the vessel to the inside surface of the inner ring, everted the vessel with minimal difficulty, and the outer ring was properly installed. Also learned in this study is that the installation of the coupler will work in scenarios when installing a vascular graft is necessary.

CHAPTER 3

SUPPORTING MATERIALS

To assist in determining which biodegradable material to use for the fabrication of the vascular coupling device, a series of tests were implemented. There are many different biodegradable materials available, and this chapter explains one in greater detail in its application to this project. Polylactic acid (PLA) is commonly used in medical applications and tissue engineering [18]. Discussed in this chapter are the fabrication and testing of PLA couplers using 3D printing, the material properties of PLA and one of its variations, and the sterilization process used to sterilize the couplers.

3.1. **Design Requirements for the Biodegradable Vascular Coupling Device**

The design requirements of the biodegradable vascular coupling device are:

- have a stiffness large enough that it won't fail when installing
- have a long enough half-life that the vessel will heal before the coupler degrades away
- be able to hold its structure in the *in vivo* environment
- not cause any negative tissue reactions as it degrades

3.2. **3D Printing**

Using the fused deposition modeling (FDM) method, 3D printed PLA couplers were fabricated, and an image of the inner and outer rings can be seen in Figure 3.1. This FDM

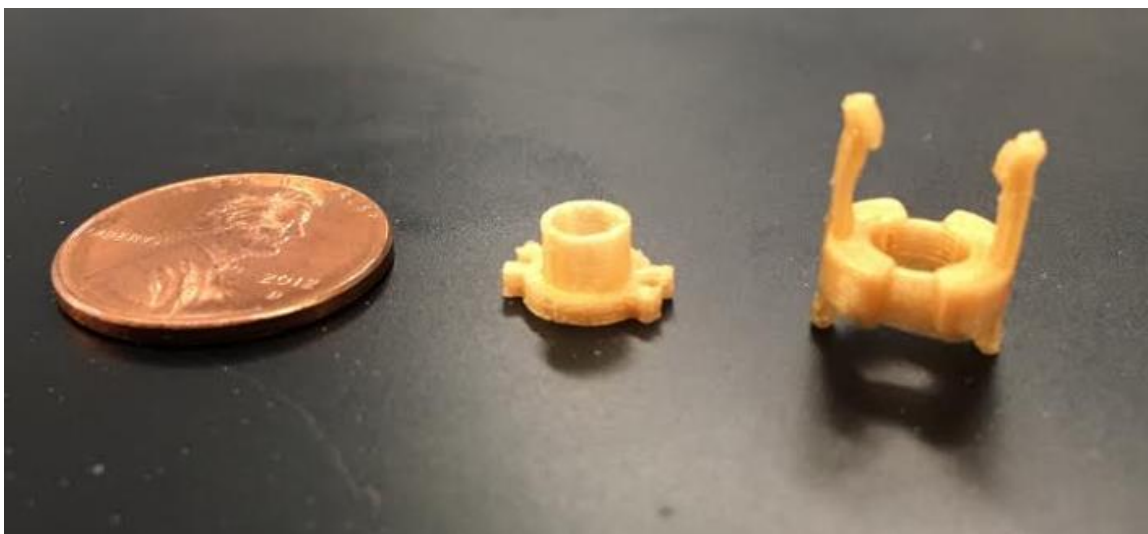


Figure 3.1: PLA inner ring (left) and outer ring (right) fabricated using 3D printing.

process is performed when thermoplastic filament is fed into a nozzle that heats up the filament so that it melts. The nozzle then ejects the melted filament onto a plate that is able to move in any direction in the XY plane while the nozzle is able to move in the Z direction. The part is then printed as the melted filament is ejected layer upon layer into the desired shape [19]. This method of fabricating is quick and relatively inexpensive; however, in the case of printing the vascular coupling device, it does not create a usable part because of its structural instability. Due to the manner in which the part is printed layer upon layer, stress concentrations result in the areas between layers of the part. Because of this stress concentration, the part is more likely to fail.

To test the functionality of the 3D printed coupler, multiple couplers were tested on the benchtop. The couplers ($n = 9$) were connected together and then pulled apart until failure. A dynamometer was used to measure the force at failure. A plot of the results can be seen in Figure 3.2. The average force at failure was 0.88 ± 0.34 N, which is a similar value to a 3 mm diameter vessel under normal physiological loading and 20% elongation (see section 2.5.2). This force at failure is also much smaller than the couplers fabricated of HDPE and PMMA, which failed at an average force of 5.52 ± 2.19 N. Also noted is the coupler failed by the arm of the outer ring snapping off on 8 of the 9 couplers. We concluded that in this case, the 3D printing method of manufacturing was a good way to visualize and get a grasp on the prototype; however, we would need a different means of manufacturing the biodegradable coupler to create a stronger coupler.

3.3. Mechanical Properties of PLA

The mechanical properties of PLA have been heavily studied as PLA is a commonly used material in tissue engineering [20]. The mechanical properties of PLA are relevant

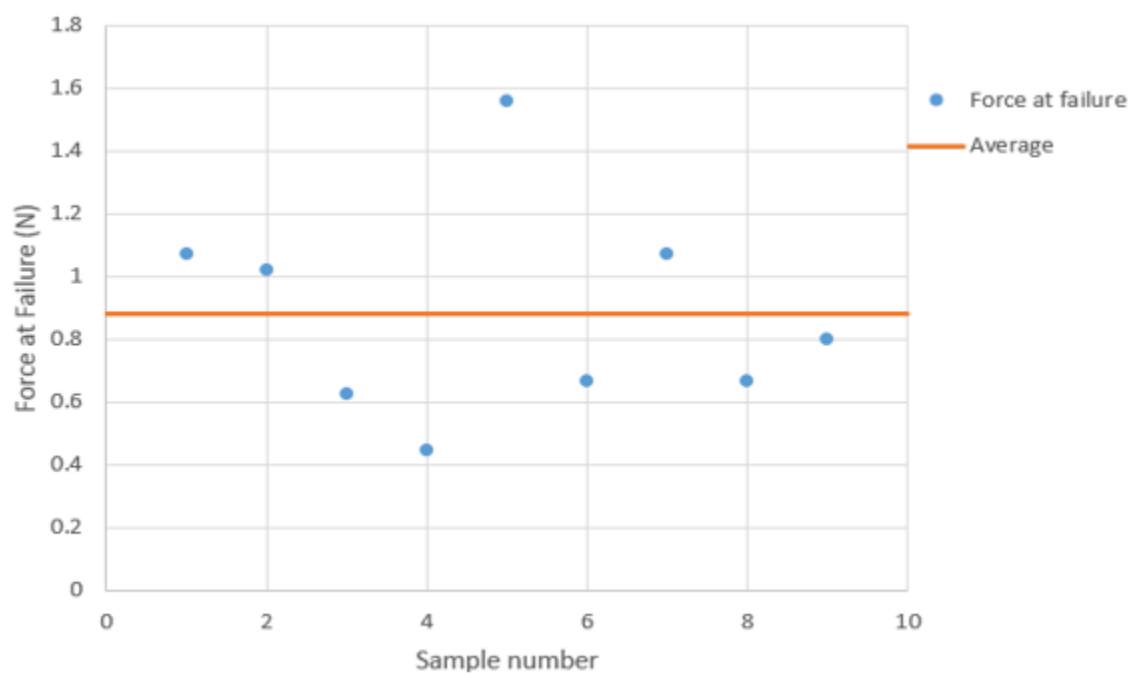


Figure 3.2: The force of the 3D printed PLA coupler at failure.

in making a consideration to what biodegradable material the vascular coupling device should be fabricated from. The glass transition temperature and melting temperature of PLA are 55°C and 180°C, respectively [21]. The degradation half-life of PLA is 6 months to 2 years depending on the isomer ratio (the ratio of L-lactic acid and D-lactic acid, the two isomers of PLA), temperature, size, and shape of the device [22]. The yield strength of PLA is approximately 30.1 MPa. Because the vascular coupling device will be implanted in the body to facilitate the healing of the vessels once anastomosed, the properties of PLA are compared to the conditions *in vivo*. The glass transition temperature is well above that of a person with a fever and high body temperature (38°C). Furthermore, a vessel will generally display perfect healing within forty-two days after the anastomosis is performed [23]. Thus, with a half-life of 6 months, the vessel will have plenty of time to heal before the coupler degrades away. Also, PLA has been shown to be well tolerated by PLA as it degrades [24]. However, the yield strength of PLA does not provide enough strength as it is estimated that the outer ring arms will experience a stress of approximately 135 MPa (APPENDIX). Therefore, a variation of PLA in which the yield strength is higher is considered.

3.3.1. Mechanical Properties of PLDLA

In order to meet the design requirements of the biodegradable vascular coupling device, the specific type of PLA that is advantageous for this project is 70/30 L/D,L PLA, also known as poly-L-D-lactic acid (PLDLA). The reason for choosing this type of PLA is that it has the mechanical properties the vascular coupling device needs once implanted into the body. Specifically, the glass transition temperature and melting temperature of PLDLA are 61.5°C and 124.5°C, respectively. The molecular weight half-life of PLDLA

is approximately 6 months [25]. The yield strength of PLDLA is approximately 424 MPa [26]. Once again, the temperature and degradation requirements are met in that the glass transition temperature is above 38°C temperature of someone with a fever, and the 6 month half-life gives the vessel enough time to heal before the coupler degrades away. In addition, the yield strength of PLDLA is significantly greater than 135 MPa (APPENDIX), resulting in a factor of safety of 3.14.

3.4. Sterilization

The method of sterilization to be used for the vascular coupling device as well as the installation tools is chosen to be STERRAD 100S. This method is chosen because its operating temperature is less than 55°C. This temperature range is acceptable because it is well below the melting temperature of both PLA and PLDLA. Also, if the material of PLDLA is selected for the vascular coupling device, the operating temperature of STERRAD 100S is below the glass transition temperature of PLDLA. Thus, the vascular coupling device will be sterilized without any concern of it losing its shape and size due to higher temperatures. The STERRAD 100S system uses hydrogen peroxide gas plasma to sterilize and its effects on different properties of polylactic acid have been shown to be negligible [27].

CHAPTER 4

CONCLUSIONS

The results of the leak tests, tensile tests, time for anastomosis, and other experiments and anastomoses provide positive results into the reliability and efficacy of the vascular coupling device with its installation tools. The following section includes conclusions that were reached throughout the project as well as future work for the project.

4.1. Conclusions

This project is a continuation of previous work done on the vascular coupling device. The goal of creating and installing a vascular anastomotic device was further achieved. Tests were performed to determine the functionality of the vascular coupling device.

The open-end leak test showed that the vascular coupling device will yield less leakage than that of a hand sutured anastomosis. The sealed-end leak test yielded results that showed that the vascular coupling device causes a lower leak rate than those vessels that are hand sutured using the running suture technique and a similar leak rate to the interrupted hand-suturing technique. These tests also demonstrated that the cadaver vessel wall will fail before the coupler will.

The tensile test showed that the vascular coupling device is able to withstand the average force vessels experience in living persons without failing, having a factor of

safety of approximately 4. The coupled vessels also performed similarly to sutured vessels, showing that there is no advantage to suturing over coupling a vessel with regards to tensile strength. Additionally, the coupler can improve its tensile strength by improving the ability to hold onto the end of the vessel, such as increasing the eversion distance of the vessel end and decreasing the space between the inner and outer rings.

The test for the speed of installation of the vascular coupling device showed that for an inexperienced individual, installing the coupler takes relatively the same amount of time for a microsurgeon to perform a running hand sutured anastomosis. However, when compared to an interrupted hand sutured anastomosis, installing the coupler is much quicker, with the interrupted suture taking approximately four times as long. Once a surgeon becomes more experienced in installing the vascular coupling device, the time for a coupled anastomosis will be significantly less than a hand sutured anastomosis with the anticipated time being under 5 minutes.

The cadaver animal study confirmed the ease of use of the installation tools when installing the vascular coupling device in a mock surgery scenario. Also learned in this study is that the coupler will function with the installation of a graft. Additionally, the importance of selecting the correctly sized coupler and anvil during installation was realized, that when sized appropriately, the installation of the coupler is very simple.

The 3D printing of the vascular coupling device yielded a good visualization of the design. Upon testing the strength of the 3D printed couplers and their ability to perform a secure anastomosis, it was learned that the 3D printed couplers will not provide the structural stability needed to hold an anastomosis intact.

In comparing the results of the testing performed on the vascular coupling device to

the desired specifications of the device from the surgeons interviewed, many of these specifications were met.

- The coupler performs a quick and reliably secure anastomosis of the blood vessels.
- The speed of the anastomosis was increased, performing it in approximately 5 minutes.
- The coupler and installation tools are intuitive in the design, allowing for an easy and simple installation.
- The coupler functions without in contact with the lumen or the blood flow.
- The coupler holds the vessel open.
- The coupler is designed to be able to work with both arteries and veins.

4.2. **Contributions**

4.2.1. Coupler Design and Fabrication

- Acquired data from many different surgeons who regularly perform vascular anastomosis. These data include difficulties that they currently experience when performing vascular anastomosis, aspects of the design that they feel the coupler needs to have, and whether or not they would use the coupler in their practice. This information was used to define and improve coupler design specifications.
- Derived the equation and calculated the critical dimensions of the inner and outer rings of the coupler. These dimensions are the length of the cylinder of the inner ring and the space between the inner and outer rings.
- Determined the size of couplers to make and test.
 - Sized for vessels of 3, 3.5, and 4 mm outer diameters.

- Designed and manufactured new tools for the installation of the vascular coupling device *in vivo*.

4.2.2. Testing

- Developed the procedure to complete the anastomosis using the installation tools.
- Constructed an enclosure to imitate a surgical incision wound opening to use in benchtop testing.
- Developed the protocol for the test to measure the time required to complete the anastomosis using the vascular coupling device and its installation tools.
- 3D printed and tested the coupler out of PLA, determining that the final product of the coupler cannot be 3D printed from PLA using the FDM printing technique.

4.3. Future Work

Future work for this project will include the manufacturing and testing of the vascular coupling device made from a biodegradable material. The biodegradable couplers should first be subjected to benchtop testing to determine the effect of degradation on the mechanical strength and dimensions over time. To evaluate the mass, dimension and tensile strength of the biodegradable couplers over time, twenty biodegradable couplers should be manufactured and put into saline to mimic the *in vivo* environment for degradation. At four different time intervals after being placed into the saline (week one, week two, week four, and week eight), five devices should be removed from the saline and a mass and dimension change test as well as a tensile strength change test should be performed. For the mass and dimension change test, the change of mass in both the inner and outer rings as well as the change in diameter and wall thickness of

both rings should be measured. For the tensile strength change, five cadaver vessels should be cut in half and anastomosed using the five coupling devices that were just pulled from the saline. A tensile test should then be performed similar to the one explained in section 2.4.2.

The next set of tests on the biodegradable couplers should be the open-end and sealed-end leak tests. This should be done to evaluate the leak proof ability of the biodegradable couplers. For each test (the open-end and sealed-end leak tests), three cadaver vessels should be cut in half and reconnected using the biodegradable coupler. For a control, three cadaver vessels that have been reconnected using a hand sutured anastomosis should be used. Leak rates should be recorded for both constant and pulsatile flows. The leak rates of the anastomotic sites should then be compared between the coupled vessels and the hand sutured vessels.

In order to evaluate the functionality of the biodegradable couplers *in vivo*, the devices should undergo a 15-day live animal study and a 90-day live animal study. For the 15-day live animal study, the biodegradable couplers should be installed on the carotid artery of a live pig (3-month-old Yorkshire cross-domestic swine; ~30 kg, n=2). A portable duplex ultrasound machine should be used postoperatively at week zero, week one, and week two to monitor the blood flow across the anastomosis. An MRI should also be used to evaluate the vessel lumen after surgery. Any changes to the biodegradable coupler and installation tools should be made if needed to refine the design and should be used for the 90-day live animal study.

The 90-day live animal study should further evaluate the performance of the biodegradable coupler. The biodegradable coupler should again be installed on the

carotid artery of a live pig (3-month-old Yorkshire cross-domestic swine; ~30 kg, n=3). Post operatively, a portable duplex ultrasound machine should be used at week zero, week one, week two, week four, week eight, and week twelve to determine the patency of the vessels. An MRI should be used to evaluate the vessel lumen after surgery. After the animals are euthanized, the coupler should be resected with approximately 1 cm of vessel on the distal and proximal end each. The coupler and vessel should then be inspected for thrombosis or intimal irregularity. The arterial anastomosis should be characterized by how well the endothelial continuity on the intima is reestablished, any degeneration, amount of sub-intimal hyperplasia (if any), and the change in the vessel diameter and wall thickness.

The tests described above should yield more concrete data on the performance of the vascular coupling device. With these data, it can be determined if fabricating the couplers out of PLDLA should function well, or if another form of PLA or other biodegradable material should be selected. These studies should drive forward the development of the biodegradable vascular coupling device and provide surgeons with a more efficient and secure option when performing vascular anastomosis.

APPENDIX

OUTER RING STRENGTH CALCULATION

To determine the strength required for the outer ring when being installed, a free body diagram is used (see Figure A.1). Because of the stress concentrations, failure will first occur at point A.

- ⇒ Need to calculate the stress σ at point A to determine the required yield strength
- ⇒ Assuming that the long arm of the outer ring can be approximated as a cantilever beam, we can use the equation for bending stress in a beam under simple bending with a stress concentration factor [28].

$$\sigma_A = k \frac{Mc}{I} \quad (\text{Equation A.1})$$

where

k = stress concentration factor

M = moment = Fd (Force time distance)

c = distance from the neutral axis (.5 mm in this case)

I = moment of inertia = $\frac{1}{12} * base * height^3$

To get the stress concentration factor, the following Figure A.2 is employed. Due to machining constraints, the fillet radius will be approximately 0.25 mm.

- ⇒ Fillet Radius / Thickness = 0.25mm / 1.0 mm = 0.25
- ⇒ Stress concentration factor $k = 2.0$

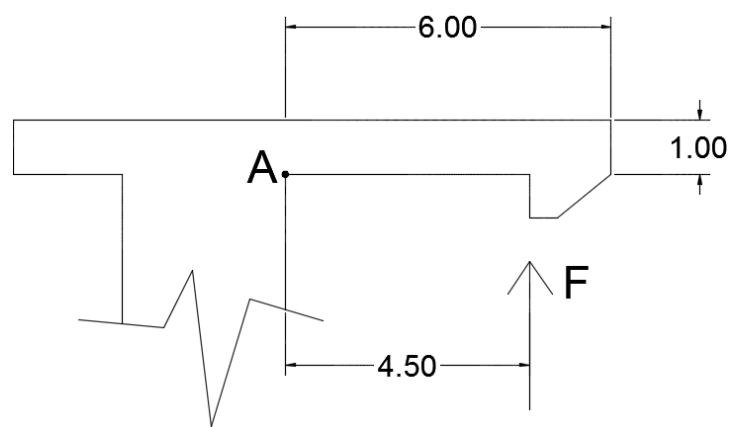


Figure A.1: Free body diagram of the outer ring when being installed.

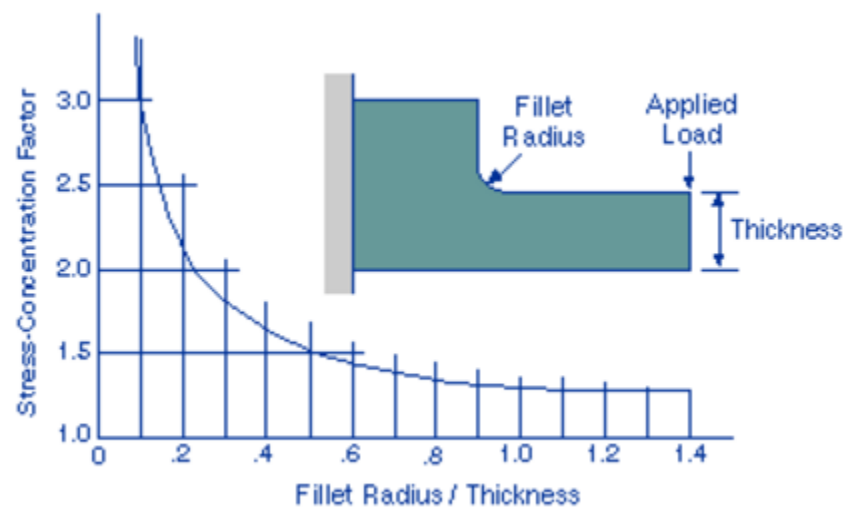


Figure A.2: Stress concentration factor chart for a cantilevered beam with a corner [29].

Now we can calculate the stress at point A, assuming the maximum force is about 15 N (this is a conservative assumption as the 15 N force is on the high end of what the outer ring arm will experience).

$$\sigma_A = 2.0 * \frac{(15N * 4.5mm) * 0.5mm}{\left(\frac{1}{12}\right) * 6mm * (1mm)^3}$$

$$\sigma_A = 135 MPa$$

REFERENCES

- [1] B. Satiani, T. E. Williams and M. R. Go, "Predicted Shortage of Vascular Surgeons in the United States: Population and Workload Analysis," *Journal of Vascular Surgery*, vol. 50, no. 4, pp. 946-952, 2009.
- [2] J. D. MacDonald, "Learning to Perform Microvascular Anastomosis," *Skull Base*, vol. 15, no. 3, pp. 229-240, 2005.
- [3] S. Jandali, L. C. Wu, S. J. Vega, S. J. Kovach and J. M. Serletti, "1000 Consecutive Venous Anastomoses Using the Microvascular Anastomotic Coupler in Breast Reconstruction," *Plastic and Reconstructive Surgery*, vol. 125, no. 3, pp. 792-798, 2010.
- [4] C. R. Davis, C. T. Rappleye, P. A. Than, M. Rodrigues, M. W. Findlay, S. N. Bishop, A. J. Whitmore, Z. N. Maan, R. B. McGoldrick, A. O. Grobbelaar and G. C. Gurtner, "Sutureless Microsurgical Anastomosis Using an Optimized Thermoreversible Intravascular Poloxamer Stent," *Plastic and Reconstructive Surgery*, vol. 137, no. 2, pp. 546-556, 2016.
- [5] M. C. Calles-Vázquez, E. A. Rubio, V. C. Ayala, J. U. Gargallo and F. M. S. Margallo, "Growing Cava Vein Anastomosis: Comparison of Cross-Clamping and Suture Times Using VCS Metallic Clips, Interrupted Nonabsorbable, or Continuous Absorbable Suturing Techniques," *Annals of Vascular Surgery*, vol. 27, no. 7, pp. 947-953, 2013.
- [6] A. B. M. Phillips, B. Y. Ginsburg, S. J. Shin, R. Soslow, W. Ko and D. P. Poppas, "Laser Welding for Vascular Anastomosis Using Albumin Solder: An Approach for MID-CAB," *Lasers in Surgery and Medicine*, vol. 24, no. 4, pp. 264-268, 1999.
- [7] C. Gehrke, H. Li, H. Sant, B. Gale and J. Agarwal, "Design, Fabrication and Testing of a Novel Vascular Coupling Device," *Biomedical Microdevices*, vol. 16, no. 1, pp. 173-180, 2014.
- [8] H. Li, C. Gehrke, B. K. Gale, H. Sant, B. Coats and J. Agarwal, "A New Vascular Coupler Design for End-to-End Anastomosis: Fabrication and Proof-of-Concept Evaluation," *Journal of Medical Devices*, vol. 9, no. 3, 2015.
- [9] H. Li, B. K. Gale, H. Sant, J. Shea and J. Agarwal, "Design, Fabrication, and Testing of a Novel End-to-end Vascular Coupling System," in *36th Annual*

- International Conference of the IEEE Engineering in Medicine and Biology Society*, Chicago, 2014.
- [10] P. B. Dobrin and T. R. Canfield, "Mechanics of Blood Vessels," in *The Biomedical Engineering Handbook, Second Edition*, Boca Raton, CRC Press, 1999, pp. 19/1-19/13.
 - [11] J. Zhou and Y. C. Fung, "The Degree of Nonlinearity and Anisotropy of Blood Vessel Elasticity," *Proceedings of the National Academy of Sciences of the United States of America*, vol. 94, pp. 14255-14260, 1997.
 - [12] Y. C. Fung and S. Q. Liu, "Determination of the Mechanical Properties of the Different Layers of Blood Vessels in vivo," *Proceedings of the National Academy of Sciences of the United States of America*, vol. 92, pp. 2169-2173, 1995.
 - [13] G. Sommer, P. Regitnig, L. K  ltringer and G. A. Holzapfel, "Biaxial Mechanical Properties of Intact and Layer-Dissected Human Carotid Arteries at Physiological and Supraphysiological Loadings," *American Journal of Physiology - Heart and Circulatory Physiology*, vol. 298, no. 3, pp. H898-H912, 2010.
 - [14] K. Takashima, R. Shimomura, T. Kitou, H. Terada, K. Yoshinaka and K. Ikeuchi, "Contact and Friction Between Catheter and Blood Vessel," *Tribology International*, vol. 40, pp. 319-328, 2007.
 - [15] E. Henrichsen, K. Jansen and W. Krogh-Poulsen, "Experimental Investigation of the Tissue Reaction to Acrylic Plastics," *Acta Orthopaedica Scandinavica*, vol. 22, no. 1-4, pp. 141-146, 1952.
 - [16] T. Khamdaeng, J. Luo, J. Vappou, P. Terdtoon and E. E. Konofagou, "Arterial Stiffness Identification of the Human Carotid Artery Using the Stress-strain Relationship In Vivo," *Ultrasonics*, vol. 52, no. 3, pp. 402-411, 2012.
 - [17] L. Xue and H. P. Greisler, "Biomaterials in the Development and Future of Vascular Grafts," *Journal of Vascular Surgery*, vol. 37, no. 2, pp. 472-480, 2003.
 - [18] K. Hamad, K. M., H. W. Yang, F. Deri and Y. G. Ko, "Properties and Medical Applications of Polylactic Acid: A Review," *Express Polymer Letters*, vol. 9, no. 5, pp. 435-455, 2015.
 - [19] I. Zein, D. W. Hutmacher, K. C. Tah and S. H. Teoh, "Fused Deposition Modeling of Novel Scaffold Architectures for Tissue Engineering Applications," *Biomaterials*, vol. 23, no. 4, pp. 1169-1185, 2002.

- [20] C. M. Agrawal and R. B. Ray, "Biodegradable Polymeric Scaffolds for Musculoskeletal Tissue Engineering," *Journal of Biomedical Materials Research*, vol. 55, no. 2, pp. 141-150, 2001.
- [21] A. Södergård and M. Stolt, "Properties of Lactic Acid Based Polymers and Their Correlation with Composition," *Progress in Polymer Science*, vol. 27, no. 6, pp. 1123-1163, 2002.
- [22] L. Xiao, B. Wang, G. Yang and M. Gauthier, "Poly(Lactic Acid)-Based Biomaterials: Synthesis, Modification and Applications," in *Biomedical Science, Engineering and Technology*, InTech, 2012, pp. 247-282.
- [23] G. Murray, "Heparin in Surgical Treatment of Blood Vessels," *Archives of Surgery*, vol. 40, no. 2, pp. 307-325, 1940.
- [24] S. Gogolewski, M. Jovanovic, S. M. Perren, J. G. Dillon and M. K. Hughes, "Tissue Response and In Vivo Degradation of Selected Polyhydroxyacids: Polylactides (PLA), Poly(3-hydroxybutyrate) (PHB), and Poly(3-hydroxybutyrate-co-3-hydroxyvalerate) (PHB/VA)," *Journal of Biomedical Materials Research*, vol. 27, no. 9, pp. 1135-1148, 1993.
- [25] M. E. R. Coimbra, C. N. Elias and P. G. Coelho, "In Vitro Degradation of Poly-L-D-lactic Acid (PLDLA) Pellets and Powder Used as Synthetic Alloplasts for Bone Grafting," *Journal of Materials Science: Materials in Medicine*, vol. 19, no. 10, pp. 3227-3234, 2008.
- [26] J. Krangas, S. Passimaa, P. Mäkelä, J. Leppilahti, P. Törmälä, T. Waris and N. Ashammakhi, "Comparison of Strength Properties of Poly-L/D-lactide (PLDLA) 96/4 and Polyglyconate (Maxon®) Sutures: In Vitro, in the Subcutis, and in the Achilles Tendon of Rabbits," *Journal of Biomedical Materials Research*, vol. 58, no. 1, pp. 121-126, 2001.
- [27] S. J. Peniston and S. J. Choi, "Effect of Sterilization on the Physicochemical Properties of Molded Poly(L-lactic Acid)," *Journal of Biomedical Materials Research*, vol. 80B, no. 1, pp. 67-77, 2006.
- [28] J. M. Gere and S. P. Timoshenko, *Mechanics of Materials*, Boston: PWS Publishing Company, 1997.
- [29] "Material Properties for Part Design," Santa Clara University, October 1998. [Online]. Available: http://www.dc.engr.scu.edu/cmdoc/dg_doc/develop/material/property/a2200002.htm#210683. [Accessed 16 January 2017].